BIOCHEMISTRY

Off-on switching of enzyme activity by near-infrared light-induced photothermal phase transition of nanohybrids

Song Zhang[1,2], Changping Wang[2], Hong Chang[1], Qiang Zhang[1]*, Yiyun Cheng[1,2]*

The off-on manipulation of enzyme activity is a challenging task. We report a new strategy for reversible off-on control of enzyme activity by near-infrared light. Enzymes acting on macromolecular substrates are embedded with an ultrasmall platinum nanoparticle and decorated with thermoresponsive copolymers, which exhibit upper critical solution temperature (UCST) behavior. The polymer-enzyme nanohybrids form microscale aggregates in solution below the UCST to prevent macromolecular substrates from approaching the enzymes and thus inhibit the enzyme activity, and they disassemble above the UCST to reactivate the enzyme. Upon near-infrared irradiation, platinum nanoparticles inside the enzymes generate heat through a photothermal effect to cause phase transition of the copolymers. Therefore, we can reversibly switch off and on the activities of three enzymes acting on polysaccharide, protein, and plasmid. The enzyme activities are increased by up to 61-fold after laser irradiation. This study provides a facile and efficient method for off-on control of enzyme activity.

INTRODUCTION

The precise control of enzyme activity is remarkably beneficial for the study of biological processes like signal transduction, gene silencing, and genome editing (*1*–*4*). Photoregulation of enzyme activity has attracted great interest owing to its unique advantages of noninvasiveness and spatiotemporal specificity (*5*–*7*), which makes it possible to manipulate an enzyme at the cellular and even molecular levels (*8*–*9*). The ideal situation for optical control of an enzyme is that the enzyme activity can be reversibly turned off and on (*10*). In nature, some proteins are sensitive to light, like rhodopsin, whose function is modulated by the cis/trans isomerization of its cofactor retinal (*11*). To enable photoinactive proteins response to light, researchers integrated photosensitive moieties like fluorescent protein domains (*12*), azobenzene analogs (*13*), *o*-nitrobenzyl moieties (*14*), and amino acids with photolabile groups (*15*) into the protein structures. Besides, they developed strategies like photosensitive molecule–driven recognition between protein and substrate and light-induced spiropyran-merocyanine transitions for the same purpose (*16*–*18*). To obtain optimal photosensitive properties, techniques including computational simulation, genetic engineering, and chemical modification were used for design and reconstruction of novel proteins (*19*, *20*), which are laborious and high cost (*21*, *22*). Moreover, high-energy lasers like ultraviolet or blue light are generally applied to activate the photosensitive moieties for optical control, which are harmful to living species and penetrate weakly in the tissues (*23*–*24*).

Nanoparticles with photothermal effect have been broadly exploited for theranostic applications (*25*, *26*). They were used for the manipulation of protein functions by near-infrared (NIR) light (*27*). For instance, Chen *et al.* (*28*) reported carbon nanotube–mediated optical activation of transforming growth factor–β, which further activated the downstream signal pathways in living cells. Singamaneni and co-workers (*27*) reported gold nanorod–associated photothermal enhancement of the activity of polymer-enzyme conjugates. A major limitation in these cases is that the protein activities cannot be reversibly manipulated. Our recent work aiming at improving the issue reported that the enzyme activities repeatedly tuned through nanoparticle-associated photothermal effect by NIR light (*29*). However, the enzyme activities could only be enhanced by two- to threefold and could not be turned off when the enzyme was not exposed to NIR light (*29*). Here, we develop a new strategy that enables off-on manipulation of the activity of enzymes acting on macromolecular substrates by NIR light. The enzyme is first used as a template to synthesize ultrasmall platinum (Pt) nanoparticle inside its structure, and then, the Pt nanoparticle–embedded enzyme (E/Pt) is decorated with a thermosensitive copolymer of acrylamide (AAm) and acrylonitrile (AN) [poly(AAm-*co*-AN)], which is an amphiphilic polymer with upper critical solution temperature (UCST) behavior in aqueous solution. The polymer-enzyme nanohybrids are insoluble at a temperature below the UCST and form microscale aggregates, which prevent macromolecular substrates from approaching the enzymes. Upon NIR irradiation, Pt nanoparticles generate heat through a photothermal effect and increase the local temperature around enzymes. As a result, the copolymer becomes soluble, and the polymer-enzyme aggregates disassemble to liberate the enzyme activity. In this study, we fabricate enzymes including glucoamylase (GA), proteinase K (ProK), and deoxyribonuclease I (DNase I) acting on starch, proteins, and DNA plasmids, respectively, into poly(AAm-*co*-AN)-engineered E/Pt (PE-E/Pt) and investigate the optical control of their enzyme activities.

RESULTS AND DISCUSSION

Design and characterization of PE-E/Pt

We fabricated the proposed PE-E/Pt by a three-step method (Fig. 1A). E/Pt is first synthesized via a chemical reduction of Pt (IV) inside of the enzyme, which is further modified with *N*-acryloxysuccinimide (NAS) on its surface to produce E/Pt-NAS. PE-E/Pt is finally obtained by copolymerization of AAm and AN on the surface of E/Pt-NAS

[1]Shanghai Key Laboratory of Regulatory Biology, School of Life Sciences, East China Normal University, Shanghai 200241, China. [2]South China Advanced Institute for Soft Matter Science and Technology, School of Molecular Science and Engineering, South China University of Technology, Guangzhou 510640, China.
*Corresponding author. Email: yycheng@mail.ustc.edu.cn (Y.C.); qzhang@bio.ecnu.edu.cn (Q.Z.)

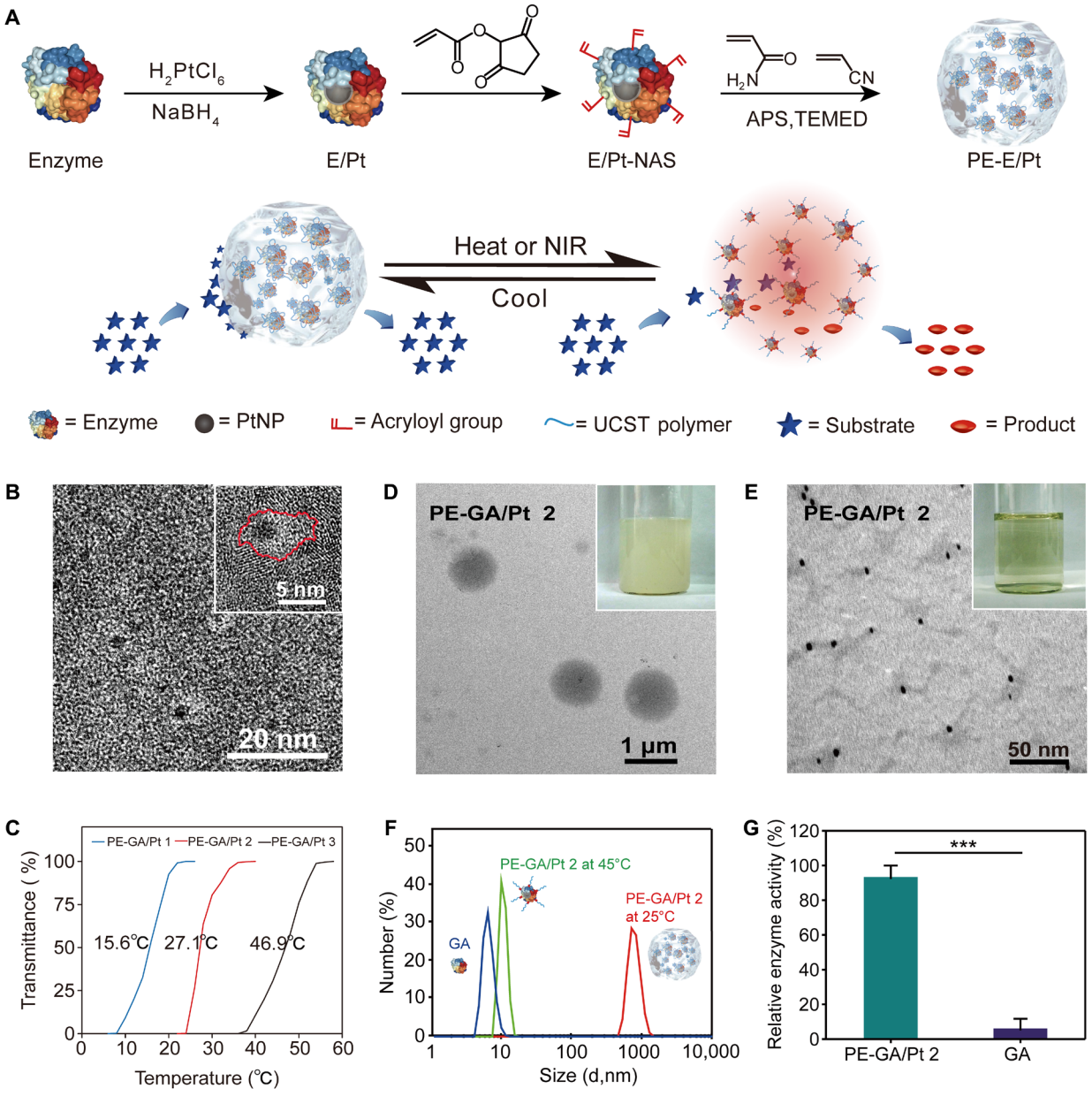

Fig. 1. Synthesis and characterization of PE-E/Pt. (**A**) Illustration depicts the synthesis of PE-E/Pt and the mechanism for off-on switching of enzyme activity by NIR light or heating. Ammonium persulfate (APS) and tetramethylethylenediamine (TEMED) were used as catalyst. (**B**) Negatively stained HRTEM image of GA/Pt. Inset is a representative GA/Pt nanoparticle, and the red line outlines the enzyme shape. (**C**) Turbidity curves of PE-GA/Pt 1, PE-GA/Pt 2, and PE-GA/Pt 3 with different phase transition temperatures. The nanohybrid concentration is 1.0 weight % (wt %). (**D** and **E**) TEM images of PE-GA/Pt 2 dropped on the grids at 25°C (D) or 45°C (E). Insets are the optical images of corresponding bulk solutions. (**F**) Hydrodynamic diameters of PE-GA/Pt 2 at 25 and 45°C. The size of GA at 25°C is used as a control. d, diameter. (**G**) Relative enzyme stability of PE-GA/Pt 2 and GA in the presence of papain. The enzyme activities of PE-GA/Pt 2 and GA were detected after incubation with papain (0.1 mg/ml) for 48 hours. ***$P < 0.001$ analyzed by Student's t test ($n = 3$). (Photo credit: Song Zhang, East China Normal University.)

(Fig. 1A) (*30*). As poly(AAm-*co*-AN) is an UCST polymer (*31*), PE-E/Pt is insoluble, forms microscale aggregates at a temperature below UCST, and becomes soluble at a temperature above the UCST, which results in an off-on switching of the enzyme activity (Fig. 1A). Enzymes acting on macromolecule substrates including GA, ProK, and DNase I are investigated in the study.

GA is an enzyme capable of hydrolyzing starch into glucose (*32*). The negatively stained high-resolution transmission electron microscope (HRTEM) image reveals that GA/Pt is highly monodispersed, and the Pt nanoparticle is inside GA. The average diameter size of Pt nanoparticles is 2.7 ± 0.5 nm (Fig. 1B), which is consistent with findings in the previous study (*33*). The circular dichroism spectra show that the secondary structure of GA is maintained in the as-prepared GA/Pt (fig. S1A). GA/Pt is then conjugated with NAS and copolymerized with AAm and AN monomers at three AN/AAm feeding molar ratios (0.5:1, 0.55:1, and 0.6:1). The as-prepared PE-GA/Pt nanohybrids are termed PE-GA/Pt 1, PE-GA/Pt 2, and PE-GA/Pt 3, respectively. The three PE-GA/Pt nanohybrids have similar weight percentages of GA (fig. S2A and table S1), and poly(AAm-*co*-AN) decorated on GA/Pt is confirmed by infrared spectrum (fig. S1B).

The phase transition temperatures of the three PE-GA/Pt nanohybrids are very different (15.6°C for PE-GA/Pt 1, 27.1°C for PE-GA/Pt 2, and 46.9°C for PE-GA/Pt 3; Fig. 1C), which should correspond to the different molar ratios of AN/AAm in the copolymers. The solution of PE-GA/Pt 2 is turbid at room temperature (below the UCST) and becomes transparent at a temperature of 45°C (Fig. 1, D and E, insets). The phase transition behavior of PE-GA/Pt 2 above the UCST is further characterized by TEM and dynamic light scattering measurement. The TEM image reveals that PE-GA/Pt 2 forms microscale aggregates at 25°C (Fig. 1D), which have a hydrodynamic diameter of 994 ± 294 nm (Fig. 1F). When the transparent solution at 45°C is added on the TEM grid, the monodispersed PE-GA/Pt 2 nanoparticles are observed (Fig. 1E), and the hydrodynamic diameter decreases to 13.3 ± 2.9 nm (Fig. 1F). These data suggest that PE-E/Pt has the thermoresponsive phase transition property in solution.

PE-ProK/Pt and PE-DNase I/Pt were also produced at the same feeding molar ratio of AAm and AN with PE-GA/Pt 2. The negatively stained HRTEM reveals that ProK/Pt and DNase I/Pt are monodispersed, and the Pt nanoparticles embedded in the enzymes have average diameters of 2.7 ± 0.4 and 2.4 ± 0.4 nm (figs. S3A and S4A). The phase transition temperatures of PE-ProK/Pt and PE-DNase I/Pt are 30.1 and 28.9°C, respectively (figs. S3B and S4B), which are close to that of PE-GA/Pt 2 (27.1°C). Furthermore, we evaluated the enzyme activities of the three enzymes before and after modification. The data show that the enzyme activities of GA, ProK, and DNase I are slightly decreased after the synthesis of Pt nanoparticles and the modification of NAS but are notably reduced after the decoration of poly(AAm-*co*-AN) (figs. S1C, S3C, and S4C). This is likely due to polymer corona on the enzyme surface retarding macromolecular substrates to reach the catalytic center of enzymes. However, the three types of PE-E/Pt nanohybrids still maintain ~40% of original enzyme activities (figs. S1C, S3C, and S4C). On the other hand, the poly(AAm-*co*-AN) effectively protects enzymes against the digestion by proteases such as papain (Fig. 1G and fig. S4D). The nanohybrids of PE-GA/Pt 2 and PE-DNase I/Pt maintain more than 95% enzyme activity after incubation with papain, while the free enzymes GA and DNase I almost lose their enzyme activities during the same period. This result suggests that the decreased enzyme activity can be compensated by much improved enzyme stability in biological systems. The improved enzyme stability after polymer modification is consistent with a previous result obtained on polymer-grafted enzymes (*34*).

Off-on switching of the enzyme activity of PE-GA/Pt

We can tune the enzyme activity of PE-GA/Pt by heating or exposure to an NIR laser (Fig. 2A). As the PE-GA/Pt nanohybrids have the thermoresponsive phase transition property, their enzyme activities should be tunable in response to temperature. To test the hypothesis, the enzyme activities of PE-GA/Pt incubated at different temperatures were investigated, and the data are shown in Fig. 2B. PE-GA/Pt 1 cannot be turned off as its phase transition temperature (15.6°C) is lower than the room temperature, while PE-GA/Pt 3 cannot be efficiently turned on due to its high phase transition temperature (46.9°C; Fig. 2B). Only PE-GA/Pt 2 is able to be turned off and on because its phase transition temperature (27.1°C) was in the range of 25 to 45°C (Fig. 2B). We also investigated the behaviors of PE-GA without Pt nanoparticles corresponding to the three PE-GA/Pt nanohybrids (termed as PE-GA 1, PE-GA 2, and PE-GA 3). The result shows that PE-GA has the similar enzyme activities with PE-GA/Pt at different temperatures (fig. S5A). Pt nanoparticle inside the enzyme can generate heat upon NIR irradiation and increase the local temperature (*29*). In our case, the PE-GA/Pt solution can be heated under NIR irradiation, and the three PE-GA/Pt nanohybrids show almost the same photothermal conversion efficiency (Fig. 2C), which indicates that NIR light can be used to manipulate the enzyme activities of PE-E/Pt. The PE-GA solutions are also irradiated by an NIR laser, but their temperatures are slightly increased (Fig. 2C). The data suggest that the increased temperature is mainly due to the photothermal effect of Pt nanoparticles. Furthermore, we evaluated the enzyme activities of PE-GA and PE-GA/Pt upon NIR irradiation. The enzyme activity of PE-GA/Pt 1 cannot be turned off at room temperature and that of PE-GA/Pt 3 cannot be turned on upon NIR irradiation (Fig. 2D). PE-GA/Pt 2 is turned off without NIR irradiation and is turned on after exposure to NIR light (Fig. 2D). The enzyme activity of PE-GA/Pt 2 is significantly enhanced when the solution temperature exceeds its phase transition temperature (fig. S5B). Last, the enzyme activity of PE-GA/Pt 2 is increased by 50-fold after laser irradiation (Fig. 2D). The three PE-GA are also irradiated by NIR light, but their enzyme activities show minimal changes in comparison with those of PE-GA without NIR irradiation (Fig. 2D). The data confirm that the photothermal effect of Pt nanoparticles takes charge of the off-on switching of enzyme activities. Moreover, the enzyme activity of PE-GA/Pt 2 can be reversibly turned off and on by NIR exposure or changing solution temperatures (Fig. 2E and fig. S5C). The enzyme activity is slightly reduced when the number of cycles increases (Fig. 2E and fig. S5C), which should be due to the heat-induced partial denaturation of enzymes. The phase transition temperatures of PE-GA/Pt are slightly increased along with their concentrations (fig. S5D), but the concentration shows minimal influence on the off-on switching of enzyme activity (Fig. 2F). Since most of the biochemical processes are carried out at a physiological temperature of 37°C, an additional PE-GA/Pt 4 was further fabricated, which has a phase transition temperature of 40.3°C (fig. S6A). The data show that the enzyme activity of PE-GA/Pt 4 is off at 37°C and can be turned on by enhancing the temperature or exposure to NIR light (fig. S6B). The result indicates that the off-on switching of enzyme activity is available under physiological conditions.

We further used PE-GA/Pt 2 for hydrogel photopatterning. In a three-enzyme cascade reaction, PE-GA/Pt 2 catalyzes the hydrolysis of starch into glucose (*32*), and then, glucose oxidase (GOx) catalyzes the oxidation of glucose to hydrogen peroxide (H_2O_2) (Fig. 3A) (*35*). Last, horseradish peroxidase (HRP) catalyzes the conversion of tetramethylbenzidine (TMB) into colored products in the presence of H_2O_2, and the color of final products could be tailored by changing the pH (Fig. 3A and fig. S7) (*36*). For photopatterning, PE-GA/Pt 2 and starch are embedded in an alginate-Ca^{2+} hydrogel, and the gel is irradiated by an NIR laser through masks to form different patterns (Fig. 3B). The abbreviation of East China Normal University (ECNU) and different geometric shapes are successfully printed on the gel upon NIR light exposure, and the colors of patterned shapes can be modulated by changing the pH (Fig. 3, C and D).

Off-on switching of the activity of PE-ProK/Pt

ProK is a serine protease to digest proteins (*37*). We further investigated the off-on control of the enzyme activity of PE-ProK/Pt (Fig. 4A). PE-ProK and PE-ProK/Pt are both tested by using casein as a substrate. Both the activities of PE-ProK and PE-ProK/Pt can

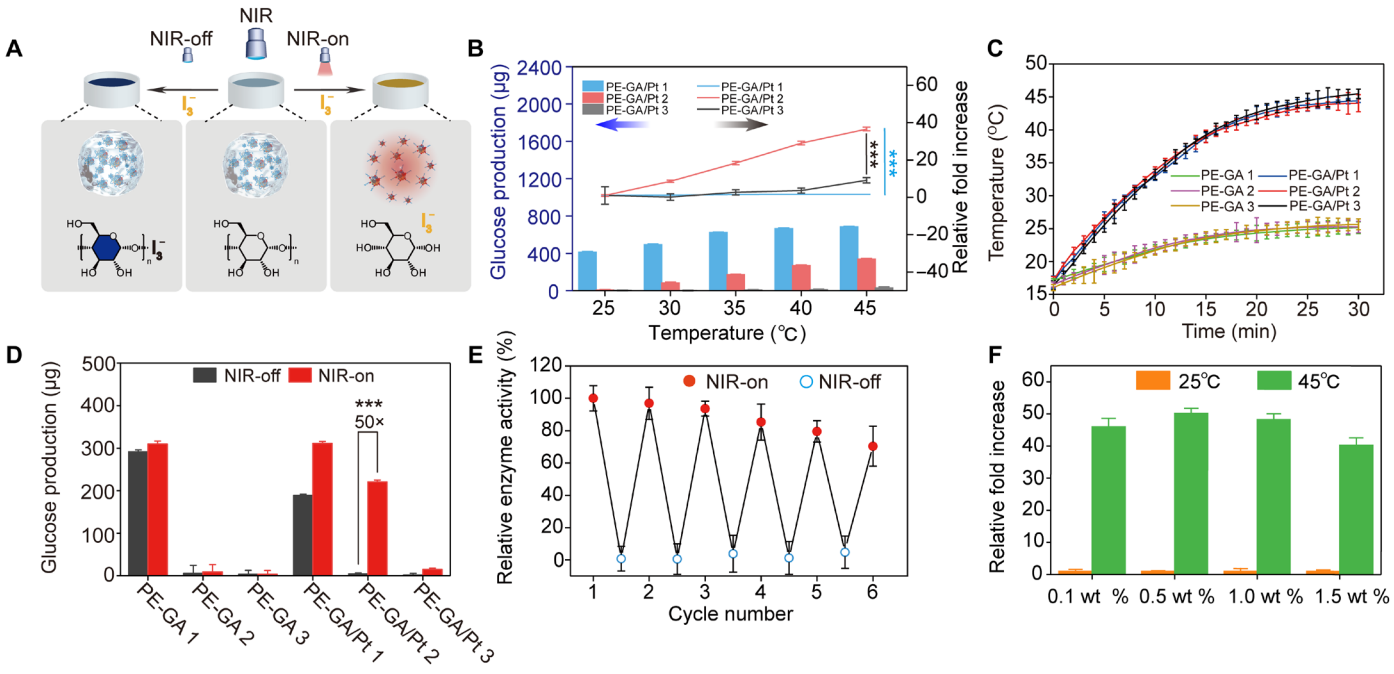

Fig. 2. Enzyme activity of PE-GA/Pt tuned by changing temperature or NIR light. (**A**) Illustration shows NIR light turns on the activity of PE-GA/Pt. PE-GA/Pt aggregates are disassembled upon NIR irradiation and recover the enzyme activity of digesting starch (the polysaccharide shown in black). Iodine (I_3^-, shown in orange) was added into the wells to stain the remaining starch, yielding blue-colored products. (**B**) Glucose production of PE-GA/Pt incubated at different temperatures for 30 min and the corresponding fold increase of enzyme activity. ***$P < 0.001$ analyzed by Student's *t* test ($n = 3$). (**C**) Temperature changes of PE-GA and PE-GA/Pt solutions upon NIR irradiation (3.8 W cm^{-2}, 30 min, $n = 3$). (**D**) Amount of glucose produced by PE-GA and PE-GA/Pt with or without NIR irradiation (3.8 W cm^{-2}, 30 min). ***$P < 0.001$ analyzed by Student's *t* test ($n = 3$). (**E**) Cycled off-on switching of the enzyme activity of PE-GA/Pt 2 by NIR light (3.8 W cm^{-2}, 30 min for each cycle, $n = 3$). (**F**) Relative fold increase of enzyme activity of PE-GA/Pt 2 at different concentrations when heated at 25 and 45°C.

be turned on by heating in water bath at 45°C, while only that of PE-ProK/Pt can be turned on by NIR irradiation (Fig. 4, B and C). Moreover, the enzyme activity of PE-ProK/Pt is increased by 22-fold upon NIR irradiation in comparison with that without laser exposure. The casein after different treatments is further analyzed by SDS–polyacrylamide gel electrophoresis (PAGE; Fig. 4D). The gel electrophoresis result reveals that casein incubated with ProK or PE-ProK/Pt and NIR irradiation are completely digested, while those treated with PE-ProK/Pt without laser exposure are not (Fig. 4D). The result suggests that the activity of PE-ProK/Pt can be switched off and on by NIR light. To visualize the off-on switching of PE-ProK/Pt activity, phycocyanin, a red fluorescent protein is used as the substrate. PE-ProK/Pt and phycocyanin are embedded in an alginate-Ca^{2+} hydrogel, and then the gel is irradiated by an NIR laser at a local region (Fig. 4E). The temperature at the NIR light–irradiated region is measured to be ~36°C (fig. S8A). The fluorescence image shows that the red fluorescence disappears in the NIR-irradiated region but remains in the non-irradiated area (Fig. 4E). For comparison, the hydrogel only containing phycocyanin is also irradiated by an NIR laser. However, the strong red fluorescence still exists in the irradiated region (fig. S8), which excludes the possibility of photobleaching. The data confirm that the enzyme activity of PE-ProK/Pt can be controlled in an off-on manner by NIR light.

Off-on switching of the activity of PE-DNase I/Pt

DNase I catalyzes the hydrolytic cleavage of phosphodiester in DNA backbone, resulting in DNA degradation (*38*). We further evaluated the NIR light–driven modulation of PE-DNase I/Pt activity (Fig. 5A). The plasmid DNA was incubated with DNase I, or with PE-DNase I/Pt plus NIR irradiation, and then analyzed via agarose gel electrophoresis. The data reveal that plasmid DNA is only degraded by PE-DNase I/Pt upon NIR irradiation (Fig. 5B). Furthermore, both PE-ProK and PE-ProK/Pt can be turned on by heating in water at 45°C (Fig. 5, C and D), which suggests that the polymer is operative. However, the activity of PE-DNase I cannot be turned on by exposure to NIR light (Fig. 5C) but that of PE-ProK/Pt can (Fig. 5D). The data are consistent with those of PE-GA/Pt and PE-ProK/Pt. Last, the activity of PE-DNase I/Pt upon NIR exposure is increased by 61-fold compared with that of PE-DNase I/Pt without NIR irradiation (Fig. 5D). Together, these results suggest that the enzyme activity of PE-DNase I/Pt can also be switched off and on by NIR light.

CONCLUSION

In summary, we fabricated poly(AAm-*co*-AN) copolymer decorated and E/Pt for off-on switching of enzyme activity by an NIR laser. The poly(AAm-*co*-AN) is a thermoresponsive copolymer with UCST behavior in aqueous solutions, and the Pt nanoparticles convert NIR light into heat to trigger the phase transition of copolymer on the enzyme surface. When the solution temperature is cooled down below the UCST, the nanohybrid PE-E/Pt forms microscale aggregates to prevent macromolecular substrates from approaching the enzymes, and thus, the enzyme activities are turned off. When the surrounding temperature is above the UCST, the enzyme activities of PE-E/Pt are turned on as the aggregates are disassembled into

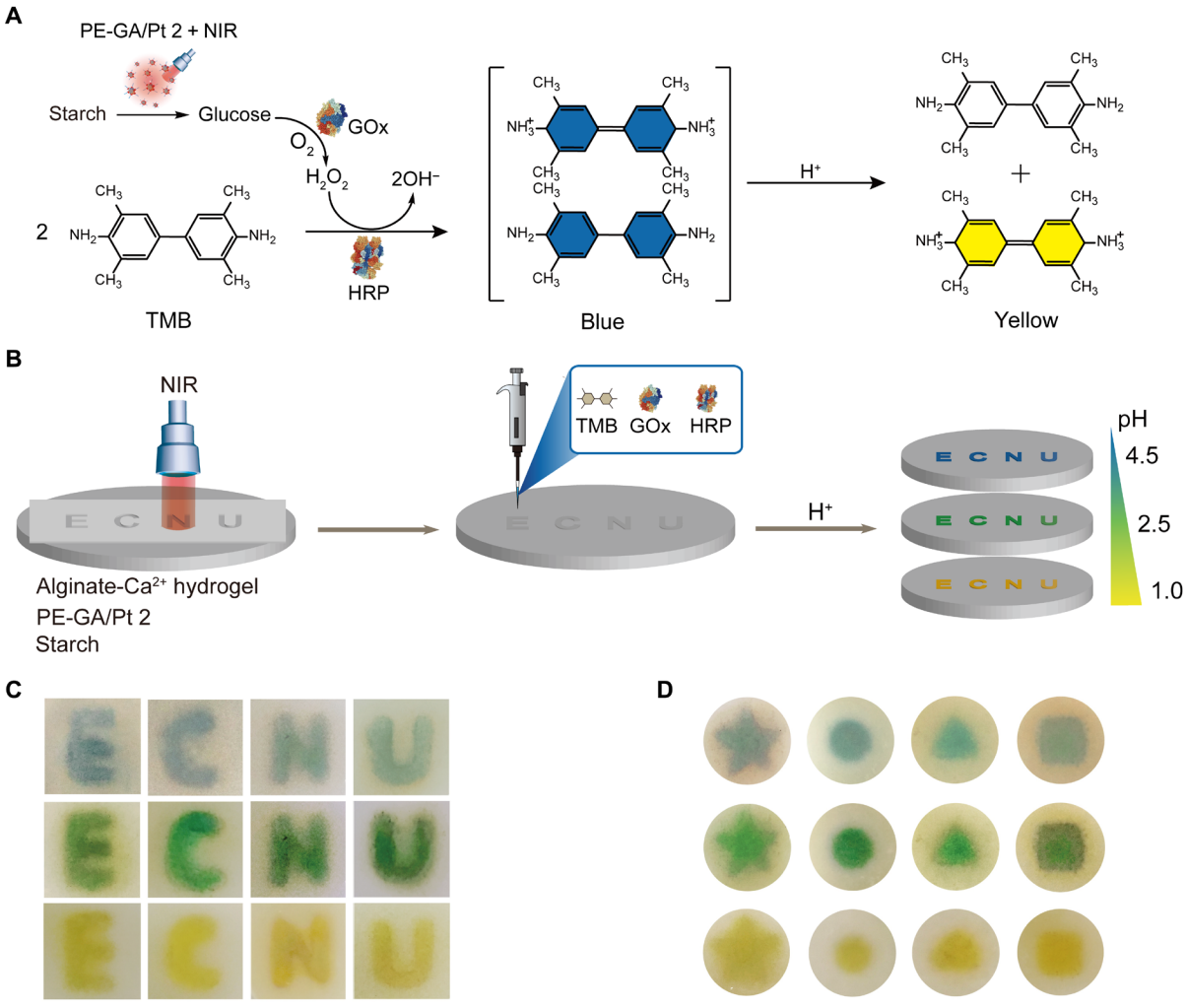

Fig. 3. PE-GA/Pt 2-associated enzymatic hydrogel photopatterning. (**A**) Scheme of the three-enzyme cascade reaction. PE-GA/Pt 2 catalyzes the degradation of starch into glucose. GOx catalyzes the oxidation of glucose to H_2O_2, and HRP catalyzes the conversion of TMB into colored products in the presence of H_2O_2. The colors are changed in response to different pH values. (**B**) Illustration of the photolithographic process. PE-GA/Pt and starch are embedded in an alginate-Ca^{2+} hydrogel. The hydrolysis reaction of starch was triggered upon NIR irradiation (3.8 W cm^{-2}, 20 min). (**C** and **D**) Abbreviation of East China Normal University (ECNU) (C) and different geometrical patterns by photolithography.

monodispersed nanoparticles. As a result, the enzyme activities of PE-E/Pt can be reversibly turned off and on by an NIR laser. A limitation of the current strategy is that only the enzymes acting on macromolecular substrates are able to be turned off, which is probably due to the fact that the copolymer poly(AAm-*co*-AN) is unable to completely prevent small-molecule substrates from reaching the enzyme below the UCST. This study provides a facile and efficient strategy to realize the off-on switching of enzyme activity via remote control by an NIR laser.

MATERIALS AND METHODS

Materials

Chloroplatinic acid hexahydrate ($H_2PtCl_6{\cdot}6H_2O$), calcium carbonate ($CaCO_3$), D-(+)-gluconic acid δ-lactone (GDL), and casein were purchased from Sigma-Aldrich (St. Louis, MO, USA). AAm and AN were purchased from Xiya Reagent (Chengdu, China). APS, TEMED, and Coomassie Brilliant Blue G250 were obtained from Macklin Biotechnology (Shanghai, China). NAS was bought from J&K Biotechnology (Beijing, China). Dimethyl sulfoxide and sodium hydroxide were purchased from Sinopharm (Shanghai, China). GA was purchased from Aike Reagent (Chengdu, China). GOx, HRP, and TMB were obtained from Yuanye Biotechnology (Shanghai, China). Starch, iodine (I_2), potassium iodide (KI), sodium thiosulfate ($Na_2S_2O_3$), sodium borohydride ($NaBH_4$), EDTA disodium salt (EDTA·2Na), magnesium sulfate ($MgSO_4$), calcium chloride ($CaCl_2$), and sodium alginate were purchased from Aladdin (Shanghai, China). ProK was obtained from Roche Diagnostics (Mannheim, Germany). DNase I was bought from Sangon Biotechnology (Shanghai, China). Sulfuric acid and hydrochloric acid were purchased from Richjoint (Shanghai, China). Uranyl acetate was purchased from Electron Microscopy China (Beijing, China).

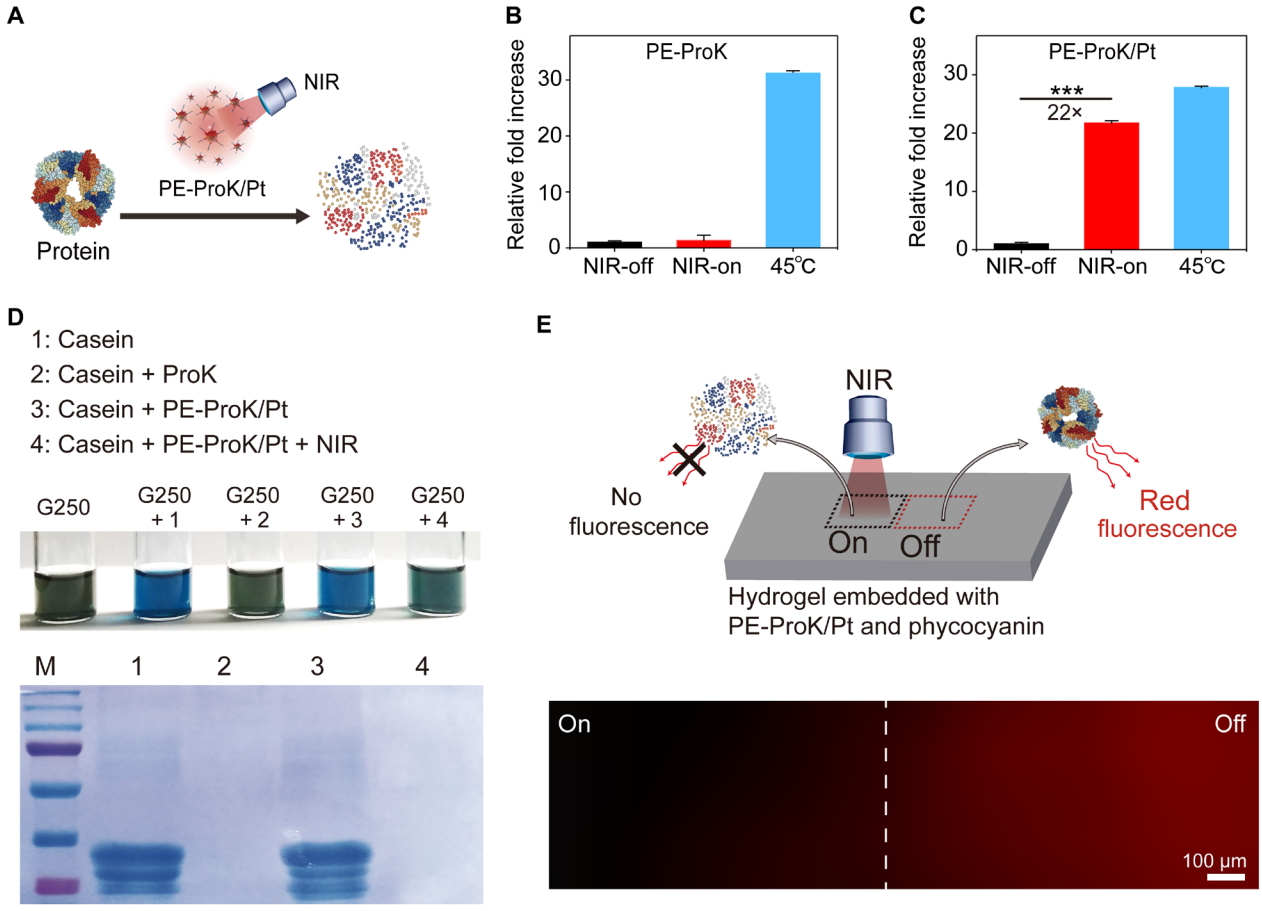

Fig. 4. Enzyme activity of PE-ProK/Pt tuned by changing temperature or NIR light. (**A**) Schematic illustrates PE-ProK/Pt catalyzes proteolysis upon NIR irradiation. (**B** and **C**) Relative fold increase of PE-ProK (B) and PE-ProK/Pt (C) activities by heating in water bath (45°C) or exposure to NIR light (3.8 W cm^{-2}, 20 min). ***$P < 0.001$ analyzed by Student's t test ($n = 3$). (**D**) SDS-PAGE of casein after different treatments (bottom). Casein is incubated with PE-ProK/Pt or ProK, and NIR irradiation (3.8 W cm^{-2}, 20 min) is applied to turn on the activity of PE-ProK/Pt. The remaining casein is stained by Coomassie Brilliant Blue G250 (top). M means protein marker (from top to bottom: 250, 150, 100, 70, 50, 35, and 25 kDa). (**E**) PE-ProK/Pt catalyzes the digestion of phycocyanin, a red fluorescent protein. The alginate-Ca^{2+} hydrogel containing PE-ProK/Pt and phycocyanin is exposed to NIR light (2.5 W cm^{-2}) for 30 min. The dashed line represents the border of laser irradiation region. (Photo credit: Song Zhang, East China Normal University.)

Synthesis of E/Pt

E/Pt was prepared according to our previous work (*29*). In a typical synthesis of GA/Pt, a mix of 5 mg of enzyme and 3 mg of $H_2PtCl_6{\cdot}6H_2O$ in 10 ml of phosphate-buffered saline (PBS) (pH 7.5) was prepared and stirred in the dark for 30 min. Subsequently, 0.25 ml of $NaBH_4$ (0.5 M) was added into the reaction solution, and the reaction was allowed to continue for 2 hours. The reaction solution was then transferred into a dialysis bag (molecular weight cutoff = 3500 Da; Biosharp) and intensively dialyzed against deionized (DI) water. The purified GA/Pt was collected and stored at 4°C for further use. The amount of GA in GA/Pt was determined by Bradford protein assay. ProK/Pt and DNase I/Pt were synthesized by the same method, except that 5 and 3 mg of $H_2PtCl_6{\cdot}6H_2O$ were added into the ProK and DNase I solutions, respectively.

Synthesis of PE-E/Pt

In a typical synthesis of PE-GA/Pt, GA/Pt was first modified with NAS. Ten milligrams of GA/Pt was dissolved in 10 ml of Hepes buffer (50 mM, pH 8.5), followed by dropwise addition of 200 μl of NAS in dimethyl sulfoxide (20 mg/ml). The reaction proceeded with magnetic stirring at 4°C for 3 hours. The product was then separated and purified via dialysis (3500 Da). The purified GA/Pt-NAS was dissolved in 10 mM PBS (pH 7.4), and then, 710 mg of AAm (10 mmol) was added to the solution. To synthesize PE-GA/Pt with different phase transition temperatures, different amounts of AN (265 mg for PE-GA/Pt 1, 292 mg for PE-GA/Pt 2, and 318 mg for PE-GA/Pt 3) were injected into the reaction solutions. For the synthesis of PE-GA/Pt 4, 20 mg of GA/Pt-NAS in 10 mM PBS (pH 7.4) was added with 710 mg of AAm and 305 mg of AN. After that, 30 mg of ammonium persulfate and 120 μl of tetramethylethylenediamine were added, and the reactions were conducted for 3 hours at room temperature. The products were collected by centrifugation (8000 rpm, 30 min) and washed 10 times by ultrapure water at different temperatures (10°C for PE-GA/Pt 1, 25°C for PE-GA/Pt 2, 45°C for PE-GA/Pt 3, and 37°C for PE-GA/Pt 4). The Pt contents in PE-GA/Pt were determined by inductively coupled plasma mass spectrometry (ICP-MS). PE-ProK/Pt and PE-DNase I/Pt were fabricated following the same protocol for the synthesis of PE-GA/Pt 2.

Negative staining of nanoparticles

Typically, 1 μl of E/Pt suspension (0.1 mg/ml) was dropped on the TEM grids using a micropipette. The droplet retained on the grid

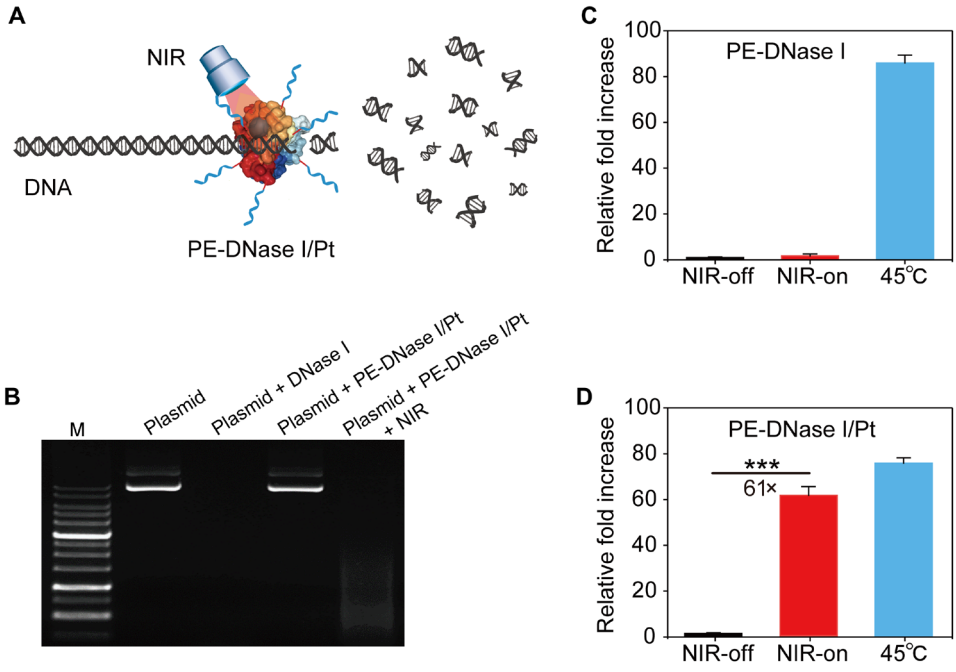

Fig. 5. Enzyme activity of PE-DNase I/Pt tuned by changing temperature or NIR light. (**A**) Illustration shows that PE-DNase I/Pt catalyzes the degradation of plasmid DNA. (**B**) Agarose gel electrophoresis of plasmid PX330 after different treatments. M means DNA marker. (**C** and **D**) Relative fold increase of PE-DNase I and PE-DNase I/Pt activities by heating in water bath (45°C) or exposure to NIR light (3.8 W cm^{-2}, 20 min). ***$P < 0.001$ analyzed by Student's t test ($n = 3$).

for 30 s, and then, a filter paper was used to absorb excess solutions. After that, 3 μl of uranyl acetate solution [1 weight % (wt %)] was dropped on the grid, and the excess solutions were absorbed from the edge of the grid using a filter paper after another 30 s. Last, the grid was placed in a clean box and air-dried for 12 hours before observation.

Characterizations

TEM images were collected on a transmission electron microscope (HT7700, Hitachi, Japan). HRTEM images were obtained by a JEM-2100F microscope (JEOL, Japan) operated at an accelerating voltage of 200 kV. The infrared spectrum was performed on a Nicolet Is50 Fourier transform infrared spectrometer (Thermo Fisher Scientific, USA) by the solid-state total reflection technique. The Pt contents in E/Pt and PE-E/Pt were determined by ICP-MS (Agilent 7500 CE, USA). The hydrodynamic diameters of nanoparticles were measured by dynamic light scattering instrument (Zetasizer Nano ZS90, Malvern Instruments, UK). The circular dichroism spectra were recorded with a J-815 spectropolarimeter (Jasco International Co., Japan).

Bradford protein assay to determine protein concentration

In a standard assay to measure GA concentration, the calibration curve of GA was first conducted. Two hundred microliters of GA solutions (50, 100, 150, 200, 250, 300, 400, 450, and 500 μg/ml) in ultrapure water were prepared, and 200 μl of ultrapure water without protein was used as blank control. Two milliliters of Bradford reagent was added into the above solutions. After 5 min, the reaction solutions (1 ml) were transferred into a 96-well plate (five wells for each sample, 200 μl per well), and then, their absorbance at 595 nm was recorded by a microplate reader (Multiskan GO, Thermo Fisher Scientific, USA). The calibration curve plotting the linear relationship for GA concentration versus the solution absorbance at 595 nm was then obtained (fig. S2). The concentrations of GA in the synthesized GA/Pt or GA/Pt-NAS were then determined. Briefly, the sample containing GA/Pt or GA/Pt-NAS was diluted by ultrapure water to obtain a solution with protein concentration in the range of 50 to 500 μg/ml. After that, the same procedure was performed as aforementioned to measure the absorbance of the sample at 595 nm. GA/Pt or GA/Pt-NAS in ultrapure water without treatment was tested as a control to exclude the influence of Pt nanoparticles in GA on the absorbance. Last, the concentration of GA in the sample was calculated according to the calibration curve. The calibration curves for ProK, casein, and DNase I were measured by a similar protocol (fig. S2), and the protein concentrations in ProK/Pt, ProK/Pt-NAS, casein, DNase I/Pt, and DNase I/Pt-NAS were calculated according to the standard curves.

Determination of the phase transition temperature of PE-E/Pt

In a typical assay, the phase transition temperatures for PE-E/Pt (1 wt %) were determined by measuring the transmittance of solution at 600 nm as a function of temperature on an ultraviolet-visible spectrophotometer (Cary 60, Agilent Technologies, USA). The temperature was controlled by circulating water. The changes in transmittance were recorded as the temperature rises. The phase transition temperature of the PE-E/Pt was defined as the temperature at which 50% change in transmittance occurred. The phase transition temperatures of PE-GA/Pt 2 at different concentrations (0.1, 0.5, 1.0, and 1.5 wt %) were also measured.

Assay for measuring the enzyme activity of PE-GA/Pt

The enzyme activity of PE-GA/Pt was determined by analyzing the remaining starch by the $Na_2S_2O_3/I_2$ titration method. GA activity is

defined as the amount of glucose generated by 1 mg of GA per hour in the presence of excess starch. In a typical assay, 10 mg of PE-GA/Pt or 0.033 mg of GA in 0.3 ml of DI water was added into 0.2 ml of sodium acetate buffer [0.05 M (pH 4.6)], and then, the reaction solution was incubated in a water bath at 25 or 45°C. Starch (2 wt %; 0.5 ml) in DI water, which was preheated in the water bath at the same temperature, was added into the reaction solution. After 30 min, 80 μl of sodium hydroxide (0.5 M) was added to terminate the reaction, and then, 0.4 ml of triiodide anion [I_3^-, 0.1 M, a mix of I_2 (13 mg/ml) and KI (35 mg/ml)] and 0.6 ml of sodium hydroxide (0.1 M) were added into the reaction solution to oxidize the generated glucose. After 15 min, 0.08 ml of sulfuric acid (2 M) was added to stop the reaction, and the remaining I_3^- in the reaction solution was measured by $Na_2S_2O_3$ titration. The amount of generated glucose by the enzymes was calculated according to titrated $Na_2S_2O_3$.

In the assay under NIR irradiation, the reaction was performed at room temperature. The mix of PE-GA/Pt and starch was irradiated by an NIR laser at 3.8 W cm^{-2} for 30 min, and then, the same procedure was conducted as described above.

Enzyme stability assay

In a typical assay, 10 mg of PE-GA/Pt 2 or 0.1 mg of GA was added into 1 ml of papain solution (0.1 mg/ml). After incubation for 48 hours, the enzyme activities of PE-GA/Pt 2 or GA were determined by using the aforementioned method. The activity of PE-GA/Pt 2 or GA in the absence of papain was measured as the control (100% relative enzyme activity). The enzyme stability of PE-DNase I/Pt and DNase I against papain was determined by the same protocol.

Cycled "off-on" switching of the enzyme activity of PE-GA/Pt

In a typical assay under heating in water bath, the mix of PE-GA/Pt 2 (10 mg/ml) and excess amount of starch (10 mg/ml) in 1 ml of sodium acetate buffer (0.01 M, pH 4.6) was prepared in centrifuge tubes. For each data point, three tubes of solutions were used, and the corresponding off-on cycles were performed. For the turn-on assay, the tubes were incubated in a water bath at 45°C for 30 min. For the turn-off assay, the tubes were incubated in a water bath at 25°C for 30 min. The reaction solution was quickly cooled down by rinsing the tubes with tap water, when converted from the incubation at 45 to 25°C. The glucose generated in each cycle was calculated by subtracting the glucose concentration before the cycle from that after the cycle. The relative enzyme activity was then calculated by using the method described in the assay for measuring the enzyme activity of PE-GA/Pt. The average enzyme activity of PE-GA/Pt at the first turn-on point was used as control (100% relative enzyme activity).

In a typical assay under NIR irradiation, the mix of PE-GA/Pt 2 (10 mg/ml) and excess amount of starch (10 mg/ml) in 1 ml of sodium acetate buffer [0.01 M (pH 4.6)] was prepared in centrifuge tubes. For the turn-on assay, three tubes were irradiated by an NIR laser (3.8 W cm^{-2}) for 30 min. For the turn-off assay, three tubes were kept at room temperature for 30 min without treatment. The cycle experiments were performed as described above.

Photolithography experiment

Typically, 7.5 mg of GDL and 4.5 mg of $CaCO_3$ were added in 1 ml of PE-GA/Pt 2 (3 wt %) aqueous suspension, and then, 10 mg of starch in 1 ml of sodium alginate (15 mg/ml) was added into the above solution to generate a hydrogel. The alginate-Ca^{2+} hydrogel containing PE-GA/Pt and starch was exposed to NIR light (3.8 W cm^{-2}) for 20 min. After that, 200 μl of a solution consisting of TMB (1 mg/ml), HRP (10 μg/ml), GOx (10 μg/ml), and 0.2 M sodium acetate buffer (pH 4.5) was added to cover the gel surface. After 10 min, 0.1 M hydrochloric acid was added to adjust the pH. Last, the gel was imaged by an optical camera.

Assay for measuring the enzyme activity of PE-ProK/Pt

The enzyme activity of ProK is defined as the amount of casein digested by 1 mg of ProK per hour. In a typical assay, 10 mg of PE-ProK/Pt in 1 ml of 50 mmol of tris-HCl buffer [containing 10 mmol of $CaCl_2$ (pH 7.5)] and 10 mg of casein were mixed, and the reaction was proceeded for 20 min at 25 or 45°C. After that, the PE-ProK/Pt in the reaction solution was removed by centrifugation (8000 rpm, 5 min) at 4°C, and the remaining casein in the supernatant was determined by the Bradford protein assay.

In the assay under NIR irradiation, the reaction was performed at room temperature. The mix of PE-ProK/Pt and casein was irradiated by an NIR laser at 3.8 W cm^{-2} for 20 min, and then, the same procedure was conducted as described above.

Assay for measuring the enzyme activity of PE-DNase I/Pt

One Kunitz unit of DNase I is defined as the amount of enzyme added to plasmid PX330 that causes an increase (0.001 per minute) in absorbance at the wavelength of 260 nm in the reaction buffer [40 mM tris-HCl, 2.5 mM $MgSO_4$, and 1 mM $CaCl_2$ (pH 8.0)]. In a typical assay, 10 mg of PE-DNase I/Pt in 0.5 ml of reaction buffer and 0.5 ml of plasmid PX330 (100 μg/ml) in reaction buffer were mixed together. The reaction was performed at 25 or 45°C for 20 min and then terminated by adding 100 μl of EDTA (20 mM). Then, the reaction solution was centrifuged (8000 rpm, 5 min) at 4°C. The absorbance of the supernatant at 260 nm was measured by NanoDrop 2000 (Thermo Fisher Scientific, USA).

In the assay under NIR irradiation, the reaction was performed at room temperature. The mix of PE-DNase I/Pt and plasmid PX330 was irradiated by an NIR laser at 3.8 W cm^{-2} for 20 min, and then, the same procedure was conducted as described above.

SUPPLEMENTARY MATERIALS

Supplementary material for this article is available at http://advances.sciencemag.org/cgi/content/full/5/8/eaaw4252/DC1

Fig. S1. Circular dichroism spectra of GA and GA/Pt, infrared spectra of poly(AAm-*co*-AN) and PE-GA/Pt 2, and enzyme activity of GA before and after modifications.
Fig. S2. Calibration curves for GA, ProK, casein, and DNase I.
Fig. S3. Negatively stained HRTEM image of ProK/Pt, turbidity curve of PE-ProK/Pt, and enzyme activity of ProK before and after modifications.
Fig. S4. Negatively stained HRTEM image of DNase I/Pt, turbidity curve of PE-DNase I/Pt, and enzyme activity and stability of DNase I before and after modifications.
Fig. S5. Enzyme activities of PE-GA at different temperatures, time-dependent glucose production by PE-GA/Pt 2 upon NIR irradiation, cycled off-on switching of the enzyme activity of PE-GA/Pt 2 by changing temperature, and turbidity curves of PE-GA/Pt 2 at different concentrations.
Fig. S6. Turbidity curve and enzyme activity of PE-GA/Pt 4.
Fig. S7. Color changes of the oxidative product of TMB at different pH values.
Fig. S8. Temperature changes of alginate-Ca^{2+} hydrogel embedded with PE-ProK/Pt during NIR irradiation and fluorescence images of phycocyanin-embedded hydrogel without and with NIR irradiation.
Table S1. The compositions of PE-GA/Pt.

REFERENCES AND NOTES

1. R. H. Kramer, A. Mourot, H. Adesnik, Optogenetic pharmacology for control of native neuronal signaling proteins. *Nat. Neurosci.* **16**, 816–823 (2013).

2. A. Berndt, S. Y. Lee, J. Wietek, C. Ramakrishnan, E. E. Steinberg, A. J. Rashid, H. Kim, S. Park, A. Santoro, P. W. Frankland, S. M. Iyer, S. Pak, S. Ährlund-Richter, S. L. Delp, R. C. Malenka, S. A. Josselyn, M. Carlén, P. Hegemann, K. Deisseroth, Structural foundations of optogenetics: Determinants of channelrhodopsin ion selectivity. *Proc. Natl. Acad. Sci. U.S.A.* **113**, 822–829 (2016).
3. L. Madisen, T. Mao, H. Koch, J.-m. Zhuo, A. Berenyi, S. Fujisawa, Y.-W. A. Hsu, A. J. Garcia III, X. Gu, S. Zanella, J. Kidney, H. Gu, Y. Mao, B. M. Hooks, E. S. Boyden, G. Buzsáki, J. M. Ramirez, A. R. Jones, K. Svoboda, X. Han, E. E. Turner, H. Zeng, A toolbox of Cre-dependent optogenetic transgenic mice for light-induced activation and silencing. *Nat. Neurosci.* **15**, 793–802 (2012).
4. J. E. Toettcher, O. D. Weiner, W. A. Lim, Using optogenetics to interrogate the dynamic control of signal transmission by the Ras/Erk module. *Cell* **155**, 1422–1434 (2013).
5. X. X. Zhou, L. Z. Fan, P. Li, K. Shen, M. Z. Lin, Optical control of cell signaling by single-chain photoswitchable kinases. *Science* **355**, 836–842 (2017).
6. L. Wang, Q. Li, Photochromism into nanosystems: Towards lighting up the future nanoworld. *Chem. Soc. Rev.* **47**, 1044–1097 (2018).
7. B. P. Timko, M. Arruebo, S. A. Shankarappa, J. B. McAlvin, O. S. Okonkwo, B. Mizrahi, C. F. Stefanescu, L. Gomez, J. Zhu, A. Zhu, J. Santamaria, R. Langer, D. S. Kohane, Near-infrared–actuated devices for remotely controlled drug delivery. *Proc. Natl. Acad. Sci. U.S.A.* **111**, 1349–1354 (2014).
8. M. J. Kennedy, R. M. Hughes, L. A. Peteya, J. W. Schwartz, M. D. Ehlers, C. L. Tucker, Rapid blue-light-mediated induction of protein interactions in living cells. *Nat. Methods* **7**, 973–975 (2010).
9. Y.-T. Lai, Y.-Y. Chang, L. Hu, Y. Yang, A. Chao, Z.-Y. Du, J. A. Tanner, M.-L. Chye, C. Qian, K.-M. Ng, H. Li, H. Sun, Rapid labeling of intracellular His-tagged proteins in living cells. *Proc. Natl. Acad. Sci. U.S.A.* **112**, 2948–2953 (2015).
10. J. Broichhagen, T. Podewin, H. Meyer-Berg, Y. von Ohlen, N. R. Johnston, B. J. Jones, S. R. Bloom, G. A. Rutter, A. Hoffmann-Roder, D. J. Hodson, D. Trauner, Optical control of insulin secretion using an incretin switch. *Angew. Chem. Int. Ed.* **54**, 15565–15569 (2015).
11. A. S. Chuong, M. L. Miri, V. Busskamp, G. A. Matthews, L. C. Acker, A. T. Sorensen, A. Young, N. C. Klapoetke, M. A. Henninger, S. B. Kodandaramaiah, M. Ogawa, S. B. Ramanlal, R. C. Bandler, B. D. Allen, C. R. Forest, B. Y. Chow, X. Han, Y. Lin, K. M. Tye, B. Roska, J. A. Cardin, E. S. Boyden, Noninvasive optical inhibition with a red-shifted microbial rhodopsin. *Nat. Neurosci.* **17**, 1123–1129 (2014).
12. X. X. Zhou, H. K. Chung, A. J. Lam, M. Z. Lin, Optical control of protein activity by fluorescent protein domains. *Science* **338**, 810–814 (2012).
13. M. Izquierdo-Serra, M. Gascón-Moya, J. J. Hirtz, S. Pittolo, K. E. Poskanzer, È. Ferrer, R. Alibés, F. Busqué, R. Yuste, J. Hernando, P. Gorostiza, Two-photon neuronal and astrocytic stimulation with azobenzene-based photoswitches. *J. Am. Chem. Soc.* **136**, 8693–8701 (2014).
14. A. Gautier, D. P. Nguyen, H. Lusic, W. An, A. Deiters, J. W. Chin, Genetically encoded photocontrol of protein localization in mammalian cells. *J. Am. Chem. Soc.* **132**, 4086–4088 (2010).
15. C. Hoppmann, V. K. Lacey, G. V. Louie, J. Wei, J. P. Noel, L. Wang, Genetically encoding photoswitchable click amino acids in *Escherichia coli* and mammalian cells. *Angew. Chem. Int. Ed.* **126**, 4013–4017 (2014).
16. J. A. Frank, D. A. Yushchenko, D. J. Hodson, N. Lipstein, J. Nagpal, G. A. Rutter, J.-S. Rhee, A. Gottschalk, N. Brose, C. Schultz, D. Trauner, Photoswitchable diacylglycerols enable optical control of protein kinase C. *Nat. Chem. Biol.* **12**, 755–762 (2016).
17. T. Tian, Y. Song, J. Wang, B. Fu, Z. He, X. Xu, A. Li, X. Zhou, S. Wang, X. Zhou, Small-molecule-triggered and light-controlled reversible regulation of enzymatic activity. *J. Am. Chem. Soc.* **138**, 955–961 (2016).
18. M. Dübner, V. J. Cadarso, T. N. Gevrek, A. Sanyal, N. D. Spencer, C. Padeste, Reversible light-switching of enzymatic activity on orthogonally functionalized polymer brushes. *ACS Appl. Mater. Interfaces* **9**, 9245–9249 (2017).
19. B. Schierling, A.-J. Noël, W. Wende, L. Thi Hien, E. Volkov, E. Kubareva, T. Oretskaya, M. Kokkinidis, A. Römpp, B. Spengler, A. Pingoud, Controlling the enzymatic activity of a restriction enzyme by light. *Proc. Natl. Acad. Sci. U.S.A.* **107**, 1361–1366 (2010).
20. E. Pastrana, Optogenetics: Controlling cell function with light. *Nat. Methods* **8**, 24–25 (2011).
21. B. Kim, M. Z. Lin, Optobiology: Optical control of biological processes via protein engineering. *Biochem. Soc. Trans.* **41**, 1183–1188 (2013).
22. F. Zhang, A. Zarrine-Afsar, M. S. Al-Abdul-Wahid, R. S. Prosser, A. R. Davidson, G. A. Woolley, Structure-based approach to the photocontrol of protein folding. *J. Am. Chem. Soc.* **131**, 2283–2289 (2009).
23. H.-Y. Youn, D. J. McCanna, J. G. Sivak, L. W. Jones, In vitro ultraviolet–induced damage in human corneal, lens, and retinal pigment epithelial cells. *Mol. Vis.* **17**, 237–246 (2011).
24. B. P. Timko, T. Dvir, D. S. Kohane, Remotely triggerable drug delivery systems. *Adv. Mater.* **22**, 4925–4943 (2010).
25. G. D. Moon, S.-W. Choi, X. Cai, W. Li, E. C. Cho, U. Jeong, L. V. Wang, Y. Xia, A new theranostic system based on gold nanocages and phase-change materials with unique features for photoacoustic imaging and controlled release. *J. Am. Chem. Soc.* **133**, 4762–4765 (2011).
26. S. Su, Y. Ding, Y. Li, Y. Wu, G. Nie, Integration of photothermal therapy and synergistic chemotherapy by a porphyrin self-assembled micelle confers chemosensitivity in triple-negative breast cancer. *Biomaterials* **80**, 169–178 (2016).
27. S. Tadepalli, J. Yim, K. Madireddi, J. Luan, R. R. Naik, S. Singamaneni, Gold nanorod-mediated photothermal enhancement of the biocatalytic activity of a polymer-encapsulated enzyme. *Chem. Mater.* **29**, 6308–6314 (2017).
28. L. Lin, L. Liu, B. Zhao, R. Xie, W. Lin, H. Li, Y. Li, M. Shi, Y.-G. Chen, T. A. Springer, X. Chen, Carbon nanotube-assisted optical activation of TGF-β signalling by near-infrared light. *Nat. Nanotechnol.* **10**, 465–471 (2015).
29. C. Wang, Q. Zhang, X. Wang, H. Chang, S. Zhang, Y. Tang, J. Xu, R. Qi, Y. Cheng, Dynamic modulation of enzyme activity by near-infrared light. *Angew. Chem. Int. Ed.* **56**, 6767–6772 (2017).
30. M. Yan, J. Ge, Z. Liu, P. Ouyang, Encapsulation of single enzyme in nanogel with enhanced biocatalytic activity and stability. *J. Am. Chem. Soc.* **128**, 11008–11009 (2006).
31. W. Li, L. Huang, X. Ying, Y. Jian, Y. Hong, F. Hu, Y. Du, Antitumor drug delivery modulated by a polymeric micelle with an upper critical solution temperature. *Angew. Chem. Int. Ed.* **54**, 3126–3131 (2015).
32. J.-z. Wang, G.-h. Zhao, Y.-f. Li, X.-m. Peng, Y.-t. Li, Biocatalytic performance of pH-sensitive magnetic nanoparticles derived from layer-by-layer ionic self-assembly of chitosan with glucoamylase. *Chem. Asian J.* **8**, 3116–3122 (2013).
33. L. Zhang, L. Laug, W. Münchgesang, E. Pippel, U. Gösele, M. Brandsch, M. Knez, Reducing stress on cells with apoferritin-encapsulated platinum nanoparticles. *Nano Lett.* **10**, 219–223 (2010).
34. Z. Gu, T. T. Dang, M. Ma, B. C. Tang, H. Cheng, S. Jiang, Y. Dong, Y. Zhang, D. G. Anderson, Glucose-responsive microgels integrated with enzyme nanocapsules for closed-loop insulin delivery. *ACS Nano* **7**, 6758–6766 (2013).
35. M. Yasuzawa, Y. Omura, K. Hiura, J. Li, Y. Fuchiwaki, M. Tanaka, Fabrication of amperometric glucose sensor using glucose oxidase-cellulose nanofiber aqueous solution. *Anal. Sci.* **31**, 1111–1114 (2015).
36. M. N. Tahir, R. André, J. K. Sahoo, F. D. Jochum, P. Theato, F. Natalio, R. Berger, R. Branscheid, U. Kolb, W. Tremel, Hydrogen peroxide sensors for cellular imaging based on horse radish peroxidase reconstituted on polymer-functionalized TiO_2 nanorods. *Nanoscale* **3**, 3907–3914 (2011).
37. D. C. Kim, Y. A. Cho, H. Li, B. C. Yung, R. J. Lee, Proteinase K-containing lipid nanoparticles for therapeutic delivery of siRNA LOR-1284. *Anticancer Res.* **34**, 3531–3535 (2014).
38. P. Sumby, K. D. Barbian, D. J. Gardner, A. R. Whitney, D. M. Welty, R. D. Long, J. R. Bailey, M. J. Parnell, N. P. Hoe, G. G. Adams, F. R. DeLeo, J. M. Musser, Extracellular deoxyribonuclease made by group A *Streptococcus* assists pathogenesis by enhancing evasion of the innate immune response. *Proc. Natl. Acad. Sci. U.S.A.* **102**, 1679–1684 (2005).

Acknowledgments

Funding: This work is financially supported by the National Natural Science Foundation of China (21725402, 31871010, and 81671822) and the Shanghai Municipal Science and Technology Commission (17XD1401600) and Guangdong Innovative and Entrepreneurial Research Team Program (2016ZT06C322). **Author contributions:** S.Z. conducted most of synthesis, characterization, and enzyme activity experiments and analyzed the data. C.W. and H.C. conducted part of the synthesis and characterization. Y.C. and Q.Z. designed and supervised the study and wrote the manuscript. **Competing interests:** The authors declare that they have no competing interests. **Data and materials availability:** All data needed to evaluate the conclusions in the paper are present in the paper and/or the Supplementary Materials. Additional data related to this paper may be requested from the authors.

Submitted 21 December 2018
Accepted 12 July 2019
Published 21 August 2019
10.1126/sciadv.aaw4252

Citation: S. Zhang, C. Wang, H. Chang, Q. Zhang, Y. Cheng, Off-on switching of enzyme activity by near-infrared light-induced photothermal phase transition of nanohybrids. *Sci. Adv.* **5**, eaaw4252 (2019).